The Astrophysical Journal Letters, 824:L1 (7pp), 2016 June 10 doi:10.3847/2041-8205/824/1/L1

HIGHEST REDSHIFT IMAGE OF NEUTRAL HYDROGEN IN EMISSION: A CHILES DETECTION OF A STARBURSTING GALAXY AT $z = 0.376$

Ximena Fernández[1,2,19], Hansung B. Gim[3], J. H. van Gorkom[2], Min S. Yun[3], Emmanuel Momjian[4], Attila Popping[5,6], Laura Chomiuk[7], Kelley M. Hess[8,9], Lucas Hunt[10], Kathryn Kreckel[11], Danielle Lucero[8], Natasha Maddox[9], Tom Oosterloo[8,9], D. J. Pisano[10], M. A. W. Verheijen[8], Christopher A. Hales[4,20], Aeree Chung[12], Richard Dodson[5], Kumar Golap[4], Julia Gross[2], Patricia Henning[13], John Hibbard[14], Yara L. Jaffé[15], Jennifer Donovan Meyer[14], Martin Meyer[5], Monica Sanchez-Barrantes[13], David Schiminovich[2], Andreas Wicenec[5], Eric Wilcots[16], Matthew Bershady[16], Nick Scoville[17], Jay Strader[7], Evangelia Tremou[7], Ricardo Salinas[7], and Ricardo Chávez[18]
[1] Department of Physics and Astronomy, Rutgers, The State University of New Jersey, Piscataway, NJ 08854-8019, USA
[2] Department of Astronomy, Columbia University, New York, NY 10027, USA
[3] Department of Astronomy, University of Massachusetts, Amherst, MA 01003, USA
[4] National Radio Astronomy Observatory, P.O. Box 0, Socorro, NM 87801, USA
[5] International Centre for Radio Astronomy Research, The University of Western Australia, Crawley, WA 6009, Australia
[6] Australian Research Council, Centre of Excellence for All-sky Astrophysics (CAASTRO), Australia
[7] Department of Physics and Astronomy, Michigan State University, East Lansing, MI 48824, USA
[8] Kapteyn Astronomical Institute, University of Groningen, Groningen, The Netherlands
[9] Netherlands Institute for Radio Astronomy (ASTRON), Dwingeloo, The Netherlands
[10] Department of Physics and Astronomy, West Virginia University, P.O. Box 6315, Morgantown, WV 26506, USA
[11] Max Planck Institute for Astronomy, Knigstuhl 17, D-69117 Heidelberg, Germany
[12] Department of Astronomy, Yonsei University, Seoul 120–749, Korea
[13] Department of Physics and Astronomy, University of New Mexico, Albuquerque, NM 87131, USA
[14] National Radio Astronomy Observatory, Charlottesville, VA 22903, USA
[15] European Southern Observatory, Alonso de Cordova 3107, Vitacura, Santiago, Chile
[16] Department of Astronomy, University of Wisconsin-Madison, Madison, WI 53706, USA
[17] Department of Astronomy, California Institute of Technology, Pasadena, CA 91125, USA
[18] Instituto Nacional de Astrofísica Óptica y Electrónica, AP 51 y 216, 72000, Puebla, México
Received 2016 January 25; revised 2016 April 27; accepted 2016 May 3; published 2016 June 2

ABSTRACT

Our current understanding of galaxy evolution still has many uncertainties associated with the details of the accretion, processing, and removal of gas across cosmic time. The next generation of radio telescopes will image the neutral hydrogen (H I) in galaxies over large volumes at high redshifts, which will provide key insights into these processes. We are conducting the COSMOS H I Large Extragalactic Survey (CHILES) with the Karl G. Jansky Very Large Array, which is the first survey to simultaneously observe H I from $z = 0$ to $z \sim 0.5$. Here, we report the highest redshift H I 21 cm detection in emission to date of the luminous infrared galaxy COSMOS J100054.83+023126.2 at $z = 0.376$ with the first 178 hr of CHILES data. The total H I mass is $(2.9 \pm 1.0) \times 10^{10} M_{\odot}$ and the spatial distribution is asymmetric and extends beyond the galaxy. While optically the galaxy looks undisturbed, the H I distribution suggests an interaction with a candidate companion. In addition, we present follow-up Large Millimeter Telescope CO observations that show it is rich in molecular hydrogen, with a range of possible masses of $(1.8–9.9) \times 10^{10} M_{\odot}$. This is the first study of the H I and CO in emission for a single galaxy beyond $z \sim 0.2$.

Key words: galaxies: evolution – galaxies: starburst – radio lines: galaxies

1. INTRODUCTION

Galaxy evolution studies have been hampered by the lack of neutral hydrogen (H I) images across cosmic time. The H I 21 cm line has been used extensively to study nearby galaxies because it is the raw fuel for star formation, it probes the internal properties, and it serves as an excellent environmental tracer (e.g., Haynes et al. 1984; Walter et al. 2008; Chung et al. 2009). Due to technical limitations, not much is known about H I in distant galaxies, but this will soon change with the next generation of radio telescopes. H I imaging at $z > 0.1$ will help constrain the evolution of the interstellar medium (ISM) and possibly explain observed phenomena at high redshift, such as the decline in the star formation rate (SFR) since $z = 2$ (Hopkins & Beacom 2006).

Over the past 15 years, several studies started to uncover the H I content beyond $z \sim 0.1$. Targeted surveys have observed H I for a limited number of galaxies at higher redshift (e.g., Zwaan et al. 2001; Catinella & Cortese 2015). Long integration times are necessary to detect H I emission from distant galaxies as the signal is very weak. As a consequence, many studies use indirect methods such as stacking and intensity mapping to attain a statistical measure of how much H I there is in the interval $z \sim 0.1$–0.8 (e.g., Lah et al. 2007; Chang et al. 2010; Delhaize et al. 2013; Geréb et al. 2013; Masui et al. 2013).

New technology now allows telescopes to carry out H I observations with large instantaneous frequency coverage. The first survey to do this is the Blind Ultra Deep H I Environmental Survey (BUDHIES), which detected H I in over 150 galaxies in and around two clusters at $0.16 < z < 0.22$ (Verheijen et al. 2007). The recently upgraded Karl G. Jansky Very Large Array (VLA)[21] can now observe the interval $0 < z < 0.5$ in one

[19] NSF Astronomy and Astrophysics Postdoctoral Fellow.
[20] Jansky Fellow of the National Radio Astronomy Observatory.
[21] The National Radio Astronomy Observatory is a facility of the National Science Foundation operated under cooperative agreement by Associated Universities, Inc.

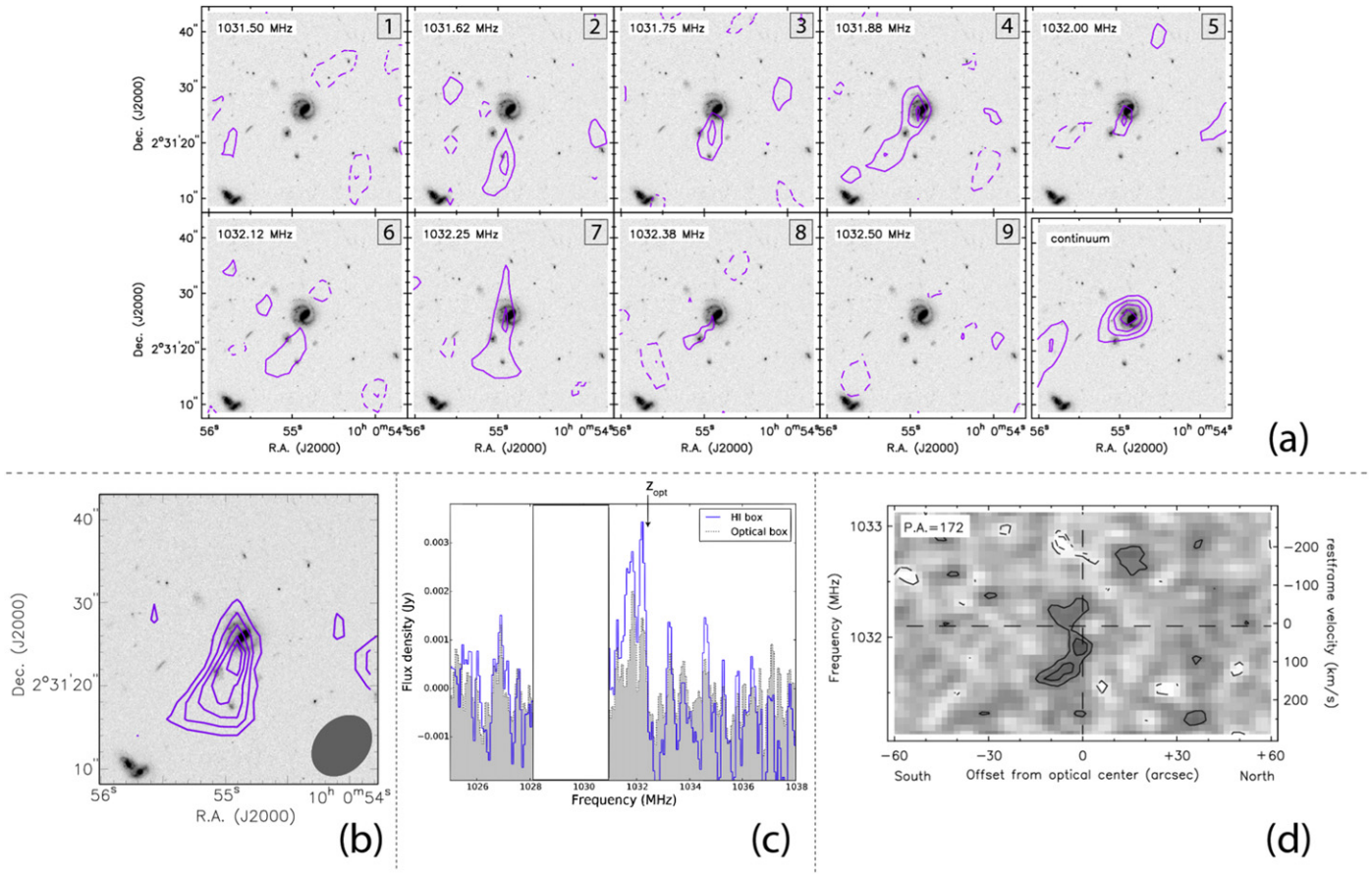

Figure 1. H I detection of J100054. (a) Channel maps showing H I contours drawn in levels of $\pm 2\sigma$, $\pm 3\sigma$, $+4\sigma$ (negative contours are dashed). The last panel shows the continuum emission for this galaxy. (b) Total H I distribution map. The ellipse shows the size of the synthesized beam ($8\farcs2 \times 6\farcs3$), and the contours correspond to (0.4, 0.9, 1.3, 1.7, 2.1) $\times$ 10^{20} atoms cm^{-2}. The background optical data is an *HST* I-band image from COSMOS (Koekemoer et al. 2007; Massey et al. 2010). (c) H I spectra integrated over the optical disk of the galaxy (gray) and over most of the H I emission (blue). The blanked region corresponds to frequencies affected by RFI and the arrow shows the frequency corresponding to the optical redshift. (d) PV diagram made through the optical center at P.A. = 172° with contours drawn in levels of $\pm 2\sigma$ and $\pm 3\sigma$. The vertical line corresponds to the optical position of the galaxy and the horizontal line corresponds to a frequency of 1032.1 MHz.

setting. We did a pilot study during commissioning that covered the interval $0 < z < 0.193$ (Fernández et al. 2013). We reached the theoretical noise over the entire frequency range, demonstrating the feasibility of an H I deep field. We are now conducting the COSMOS H I Large Extragalactic Survey (CHILES) with the VLA, a 1002 hr survey where we expect to directly image the H I distribution and kinematics of at least 300 galaxies in the COSMOS field from $z = 0$ to $z \sim 0.5$, with at least 200 of these at $z > 0.2$. These estimates are done by comparing our 5σ sensitivity curve (assuming a 150 km s^{-1} width) with the H I masses predicted for spectroscopically confirmed galaxies in the observed volume using the scaling relation from Catinella et al. (2012).

Here, we report the H I detection of the Luminous Infrared Galaxy (LIRG) COSMOS J100054.83+023126.2 (henceforth J100054) at $z = 0.376$ with the first 178 hr of CHILES data. In addition, we include CO observations from the Large Millimeter Telescope Alfonso Serrano (LMT) and follow-up optical spectroscopic data that confirm the redshift of the detection. This study not only represents the highest redshift H I detection in emission, but it is the first time we can study the cold gas content (both molecular and atomic hydrogen) of a galaxy at $z > 0.2$.

This letter adopts $H_o = 70$ km s^{-1} Mpc^{-1}, $\Omega_M = 0.3$, and $\Omega_\Lambda = 0.7$, and a Kroupa (2001) initial mass function.

2. OBSERVATIONS AND RESULTS

2.1. Cold Gas Properties

2.1.1. CHILES: H I Detection at $z = 0.376$

We are observing one pointing in the COSMOS field with the B configuration of the VLA, which corresponds to a spatial resolution of ~25 kpc at $z = 0.376$. The first 178 hr (Phase I) were observed in 2013 (E. Momjian et al 2016, in preparation).

For this preliminary study we imaged the interval $0.36 < z < 0.39$ (1025–1045 MHz), which includes a wall with over 250 galaxies with spectroscopically known redshifts, and 60 of these have predicted $M_{\rm H\,I} > 10^{10} M_\odot$. The cube was made with a robustness parameter of 0.8 in CASA, it has a spatial scale of 2048 $\times$ 2048 of $2''$ pixels, and a total of 320 channels of 62.5 kHz (18 km s^{-1} at $z = 0.376$). We first Hanning smoothed the data to increase the signal-to-noise ratio (S/N) and then iteratively subtracted the continuum in the image plane, leading to a typical noise per channel of 75 μJy beam^{-1}. We searched for H I by eye around a subset of the 60 predicted gas-rich galaxies. We are still in the process of searching for H I around other galaxies directly and via stacking.

We detect H I in the galaxy J100054, which has a predicted $M_{\rm H\,I} = 2.8 \times 10^{10} M_\odot$. The H I channel maps (Figure 1(a)) show that the emission is mostly at the 2–3σ level (with a 4σ peak at the position of the galaxy). Although the emission is

weak, we trust the detection because the signal is at the location and velocity of the galaxy and it appears in several consecutive independent channels. The emission is seen in seven panels, making it 875 kHz wide, which translates to a velocity width of 246 ± 36 km s^{-1} after correcting for the channel width. We calculate $z_{\rm H\,I} = 0.3764 \pm 0.0002$, assuming that the center of the emission is that shown in Figure 1(a), panel 5. We have high confidence in the emission seen in panels 2–5, as it is at the 3σ level with a smooth velocity gradient and there are no negative contours of high significance. The emission in panels 6–8 is weaker and its velocity does not follow a clear pattern. We generate the total H I distribution map (Figure 1(b)) by adding the emission seen in the seven channels after smoothing and applying a 1.25σ cutoff. We also make a moment map excluding the emission seen in panels 6–8, and the morphology is almost identical. We calculate $M_{\rm H\,I}$ for both maps, $M_{\rm H\,I} = (2.9 \pm 1.0) \times 10^{10}\,M_\odot$ for the one presented here and $M_{\rm H\,I} = 2 \times 10^{10}\,M_\odot$ from the map only including panels 2–5, showing that the H I in panels 6–8 does not contribute much. As seen in Figure 1(b), the H I is asymmetric and very extended, encompassing some potentially nearby companions. Because the low-level emission in the southern extension is rather sensitive to the noise, the morphology is uncertain. We also include two integrated H I spectra in Figure 1(c), one that integrates over the optical disk of the galaxy and another one that is centered on the H I emission. We calculate a S/N = 7 from the H I spectrum by adding up the signal in the range 1031.5–1032.5 MHz, and dividing by the rms calculated in the range 1033–1038 MHz (taking into account the number of channels). Last, Figure 1(d) shows a position–velocity diagram that further shows the significance of the detection.

The last panel of Figure 1(a) (bottom right) shows the continuum emission from the line-free channels. In addition, we have continuum data from the commensal survey CHILES Continuum Polarization (CHILES Con Pol).[22] The source has a total flux density of 240 ± 10 μJy at 1.45 GHz, which is consistent with our measurement and the COSMOS-VLA data (Schinnerer et al. 2007). We measure a spectral index of −0.8 ± 0.15, which is the typical value for star-forming galaxies (e.g., Magnelli et al. 2015).

2.1.2. CO Observations with the LMT

As a follow-up to our H I detection, we observed J100054 using the Redshift Search Receiver (RSR) at the LMT (Erickson et al. 2007) on 2015 April 8 and May 21 for 1 hr each under excellent weather conditions ($T_{\rm sys} \equiv 100$ K). The spectrum covering a frequency range 73–111 GHz is obtained with a spectral resolution of 31.25 MHz (∼110 km s^{-1} at $z = 0.376$) to search for possible CO(1–0) emission. The effective beam size is 25″ at 84 GHz and telescope pointing is checked on the nearby QSO J0909+013 before each observing session. When averaged together with the $1/\sigma^2$ weight, the final spectrum has an rms noise of $\sigma = 1.2$ mJy.

A single bright line is detected with a S/N = 9.7 centered at 83.7816 GHz (Figure 2) and is interpreted as that of the CO(1–0) transition at $z = 0.3759 \pm 0.0002$. This line is fully resolved, as shown by the zoom-in spectrum shown in the inset, and the derived full width at half maximum (FWHM) is 413 ± 62 km s^{-1} after correcting for the instrumental resolution. The narrow CO line peak (FWHM is 317 ± 56 km s^{-1}), centered on

[22] http://www.chilesconpol.com

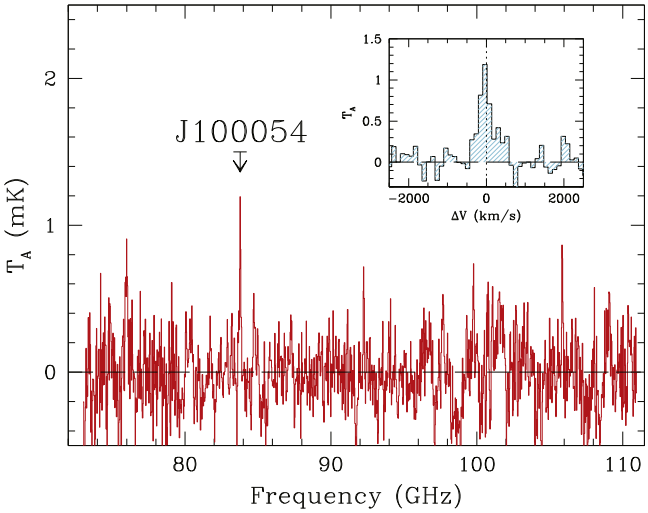

Figure 2. CO spectrum for J100054 obtained using the RSR on the LMT. The larger panel shows the full frequency range and the inset shows a zoom-in on the CO(1–0) detection at 83.7727 GHz ($z = 0.376$).

the optical redshift $z = 0.376$, sits atop a broad base, which accounts for the observed broadline width. The measured CO line integral of 3.12 ± 0.32 Jy km s^{-1} translates to $L_{\rm CO} = (2.3 \pm 0.2) \times 10^{10}$ K km s^{-1} pc^2. The H_2 mass depends on the adopted conversion factor, which ranges from $\alpha = 0.8\,M_\odot/$(K km s^{-1} pc^2) for interacting galaxies (Downes & Solomon 1998) to the Galactic conversion factor of $\alpha = 4.3\,M_\odot/$(K km s^{-1} pc^2) (Bolatto et al. 2013). This results in a range of possible values of $M_{\rm H_2} = (1.8\text{–}9.9) \times 10^{10}\,M_\odot$.

2.2. Additional Data

2.2.1. COSMOS Multiwavelength Data

As J100054 is located within the COSMOS field, extensive multiwavelength data are available, and it is detected in ultraviolet, optical, IR, and by the VLA-COSMOS continuum survey. A deep *HST* I-band image of J100054 (Figure 3(a)) shows that it is a massive regular barred spiral with clear spiral arms and a prominent bulge. In addition it shows a number of fainter galaxies, suggesting that this may be a small group. The information for the possible companions is scarce, as the four are very faint with $r > 23$ and only have measured photometric redshifts. Only one of the companions has a photometric redshift similar to J100054, but spectroscopic data are necessary to confirm this and determine whether the other ones are indeed background objects.

2.2.2. Optical Spectroscopic Confirmation

We obtained an additional long-slit spectrum with the SOAR 4.1 m telescope and the Goodman High Throughput Spectrograph on 2015 April 17 to confirm the redshift of J100054. A slit of 1.″68 width was oriented north–south on the galaxy and the 400 l mm^{-1} grating yielded spectral coverage 3500–7500 Å at a resolution of $R = 495$. The 1 hr exposure confirms a galaxy at $z = 0.3758 \pm 0.0001$ with strong [O II] 3727 Å emission and Balmer absorption, indicating a post-starburst stellar population. The spectrum shows no signs of AGN activity, as seen in Figure 3(b).

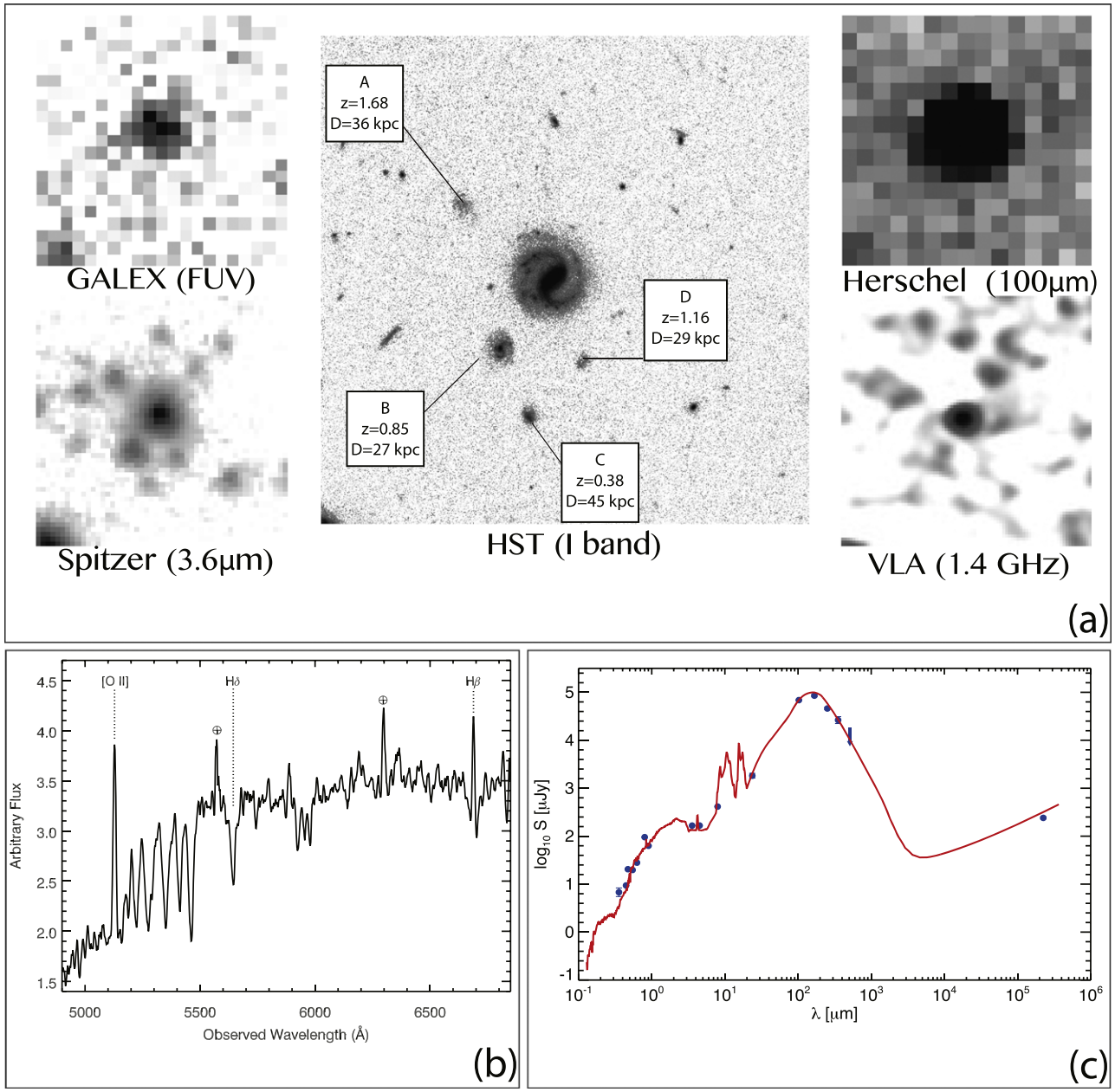

Figure 3. Multiwavelength data for J100054. (a) Images of J100054 detected with different telescopes: *GALEX*, *Spitzer*, *HST*, *Herschel*, and the VLA (all are $30'' \times 30''$). The central image is labeled with possible companions, their photometric redshift, and projected distance from the main galaxy (assuming they are at the same redshift). (b) Optical spectrum that confirms the redshift of the galaxy. The different lines are labeled and the Earth symbols correspond to prominent sky lines. (c) SED fit using the available photometry.

2.2.3. Spectral Energy Distribution (SED) Fitting

The optical and IR counterparts are found exploiting the likelihood ratio technique (Sutherland & Saunders 1992) with the optical photometric data (Capak et al. 2007), *Spitzer Space Telescope* MIPS 24 μm (Le Floc'h et al. 2009), and the *Herschel Space Observatory* (Oliver et al. 2010; Lutz et al. 2011). The best-fit SED is obtained through the *Le Phare* (Arnouts et al. 1999; Ilbert et al. 2006) with the M82 galaxy template for the optical-mid IR regime and the Chary–Elbaz galaxy template for the far-IR regime at the fixed redshift of $z = 0.37$. The best-fit SED yields the total $L_{\rm IR}(8\text{–}1000\,\mu{\rm m}) = (5.7 \pm 0.4) \times 10^{11}\,L_{\odot}$ and the $L_{\rm FIR}(40\text{–}120\,\mu{\rm m}) = (3.0 \pm 0.2) \times 10^{11}\,L_{\odot}$, confirming that this object is a LIRG.

2.2.4. Stellar Mass and SFR Estimate

We compute $M_{*} = (8.7 \pm 0.1) \times 10^{10}\,M_{\odot}$ using the *Spitzer* IRAC data (Eskew et al. 2012). Following Murphy et al. (2011), we calculate the SFR using the FUV, IR, and radio data $\mathrm{SFR_{FUV}} = (0.7 \pm 0.1)\,M_{\odot}\,\mathrm{yr^{-1}}$, $\mathrm{SFR_{IR}} = (85 \pm 6)\,M_{\odot}\,\mathrm{yr^{-1}}$, and $\mathrm{SFR_{1.4\,GHz}} = (72 \pm 3)\,M_{\odot}\,\mathrm{yr^{-1}}$ (errors come from the photometric uncertainties). The $\mathrm{SFR_{FUV}}$ is negligible, indicating that most of the star formation is dust-obscured. We adopt $\mathrm{SFR_{IR}}$ for the rest of the paper.

3. DISCUSSION

3.1. Unusual Spiral Galaxy

While the optical image shows J100054 to be a large normal spiral, the cold gas properties depict a more complex picture.

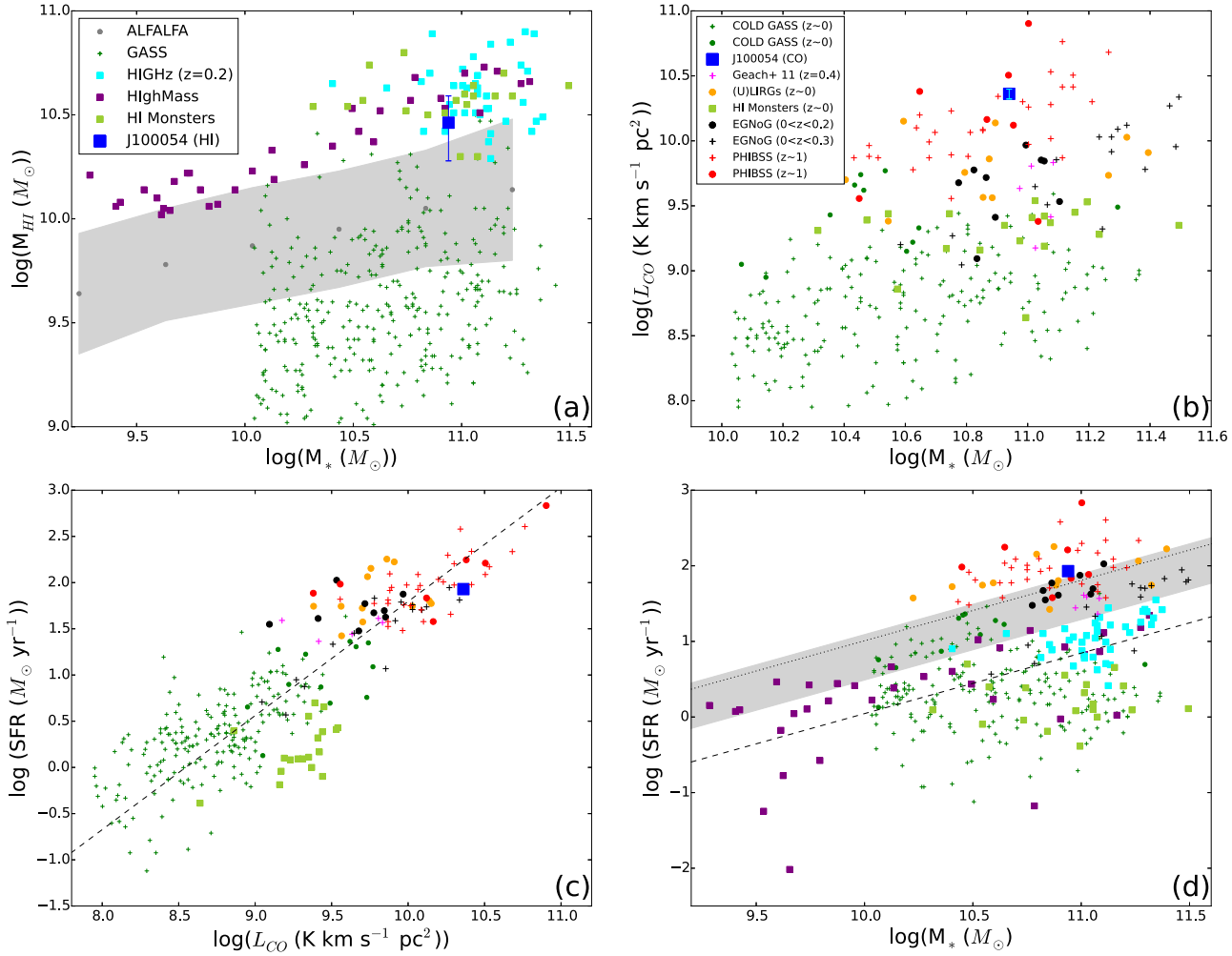

Figure 4. Properties of J100054 compared with other surveys. The different colors correspond to blue (the results presented here), gray (ALFALFA; median and 1σ values for each bin from Maddox et al. 2015), purple (HighMass selected from ALFALFA; Huang et al. 2014), yellow–green (H I monsters; Lee et al. 2014), cyan (HIGHz; Catinella & Cortese 2015), green (GASS and COLD GASS; Saintonge et al. 2011; Catinella et al. 2012), magenta (Geach et al. 2011), orange (CO from Gao & Solomon 2004, M_* and SFR from U et al. 2012), black (EGNoG; Bauermeister et al. 2013), and red (PHIBSS; Tacconi et al. 2013). The filled circles represent mergers, starbursts and/or ULIRGs, the plus signs correspond to normal star-forming galaxies, and the squares are unclassified. The different redshifts are noted in the legends. All of the numbers shown here are calculated using the same cosmology and Kroupa IMF. The $L_{\rm CO}$ correspond to CO(1-0) observations except for PHIBSS that observed CO(3-2), but we convert to CO(1-0) assuming CO(1-0)/CO(3-2) = 2. (a) $M_{\rm H\,I}$ vs. M_*. (b) $L_{\rm CO}$ vs. M_*. (c) SFR vs. $L_{\rm CO}$. The dashed line corresponds to the correlation between $L_{\rm CO}$ and $L_{\rm IR}$ for normal star-forming galaxies (Sargent et al. 2014). (d) SFR vs. M_* compared with the SFR–M_* relation at different redshifts from Bauermeister et al. (2013). The shaded region corresponds to $z = 0.376$, with the lower bound showing the SFR–M_* relation at that z and the upper bound indicating the starburst threshold. The relations at $z = 0$ (dashed line) and at $z = 1$ (dotted line) are included for reference.

The H I mass agrees with the predicted one, but its distribution and kinematics are unexpected. The H I suggests the possibility of a gravitational interaction, as the H I looks very disturbed. Many studies have reported SFR enhancement in interacting pairs. In particular, in the case of a minor merger, the more massive companion experiences a stronger SFR enhancement than the less massive one (e.g., Scudder et al. 2012; Davies et al. 2015). Spectroscopic data are necessary to determine whether the nearby galaxies are at the same redshift.

In addition, the galaxy is extremely H_2 rich, with a value that is even unexpected for local (U)LIRGs. The $L_{\rm CO}$ for this system is approximately six times higher than objects with similar $L_{\rm IR}$ in a sample of local (U)LIRGs (G. Privon 2016, in preparation). Here, we present a range of possible values for $M_{\rm H_2}$ (depending on α), but we note that $\alpha = 0.8$ is still a matter of debate even for extreme (U)LIRGs such as Arp 220 (Scoville et al. 2015). The CO spectrum suggests there might be two components: a broad one and a narrow one. The FWHM of the narrow component is consistent with the H I width within the uncertainties. The broad component could be emission from neighboring galaxies included in the large beam. We note, however, that the galaxies are fairly small and we do not expect significant contribution. The more likely explanation is an outflow such as those seen for local (U)LIRGs (e.g., Chung et al. 2011).

3.2. Comparison with Other Samples

Figure 4 explores whether the gas properties are unusual for a galaxy with that M_* and SFR when compared with the properties of galaxies found in other surveys (see the caption for details and references). Figure 4(a) compares the H I mass and M_* of J100054 to systems found in other surveys. As seen, J100054 is rich in atomic gas when compared with ALFALFA and GASS, and in fact has as much H I as the most H I -rich galaxies at $z \sim 0$–0.2. Figure 4(b) shows $L_{\rm CO}$ (instead of H_2 mass to avoid issues with α) as a function of M_*. The plot

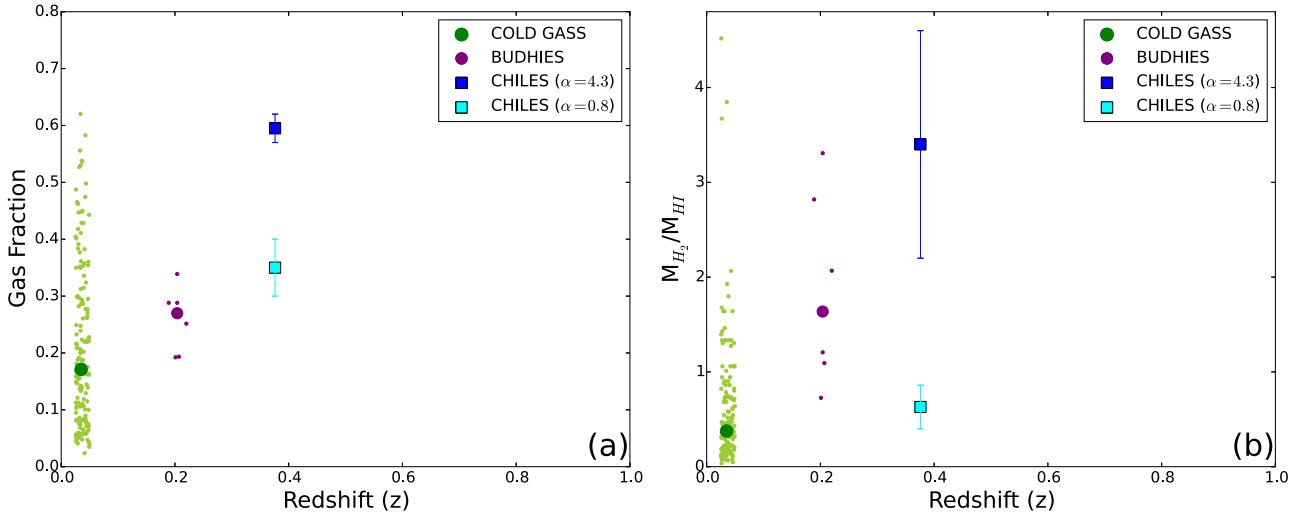

Figure 5. ISM properties at different redshifts for three surveys: COLD GASS, BUDHIES, and CHILES. We include all of the galaxies with detected H I and H_2 for the first two surveys, with the bigger symbol showing their median value. (a) Gas fraction ($(M_{\rm H\,I} + M_{\rm H_2})/(M_{\rm H\,I} + M_{\rm H_2} + M_*)$) vs. redshift. (b) H_2/H I ratio vs. redshift.

shows that most galaxies have lower $L_{\rm CO}$, while only those at $z \sim 1$ have comparable values to J100054. The third plot shows SFR as a function of $L_{\rm CO}$ (Figure 4(c)). This is usually plotted as $L_{\rm IR}$ versus $L_{\rm CO}$, but here we choose SFR as some of the samples do not have published $L_{\rm IR}$. From this plot we can infer that J100054 has a relatively low star formation efficiency because it lies below the line that marks the SFR–M_* relation (commonly known as the "main sequence"). Last, we look at the SFR for different M_* (Figure 4(d)). J100054 is just above the starburst threshold, which is defined as four times the SFR–M_* relation (Rodighiero et al. 2011). In summary, these four plots show that J100054 is gas-rich both in molecular and atomic gas, but its SFR is somewhat low given its $L_{\rm CO}$.

3.3. ISM Studies at Intermediate Redshift

Finally, we emphasize this is the first time we observe both the CO and H I from a galaxy beyond the local universe ($z \sim 0.2$). In Figure 5 we show how the gas fraction and $M_{\rm H_2}/M_{\rm H\,I}$ ratio vary with redshift for three surveys: COLD GASS, BUDHIES (Verheijen et al. 2007; Cybulski et al. 2016), and CHILES. These limited data suggest that if we assume $\alpha = 4.3$, both the gas fraction and ratio of H_2/H I go up with increasing redshift and that J100054 is above the median seen in surveys at $z = 0$ and $z = 0.2$. If we adopt $\alpha = 0.8$, the gas fraction is still high when compared with other surveys, but the mass ratio is comparable to galaxies at $z = 0$. We cannot draw strong conclusions with only one data point, but we will soon be able to start populating these plots with upcoming CHILES results and follow-up observations with the LMT. This will be further complemented by the upcoming surveys that will be conducted with ALMA, and the SKA and its precursors in the next decade.

In addition to probing the general galaxy population, we can also start to probe the evolution of (U)LIRGs. We know that these systems correspond to mergers in the local universe, but there is disagreement on the merger contribution at higher redshifts (e.g., Kartaltepe et al. 2010). Future H I and H_2 data will allow us to understand these systems better and probe their ISM across cosmic time.

4. SUMMARY

We presented the first comprehensive study of the gas content (H I and H_2) of a galaxy at intermediate redshifts. We summarize our main findings below.

1. We detected the highest redshift H I in emission to date from a very gas-rich system ($M_{\rm H\,I} = (2.9 \pm 1.0) \times 10^{10}\,M_\odot$). Its H I mass is similar to the most gas-rich galaxies locally known and consistent with what is expected from its stellar properties.
2. J100054 is also gas-rich in H_2, with a mass range of $(1.8–9.9) \times 10^{10}\,M_\odot$. The CO luminosity is higher than what is expected for a galaxy with that stellar mass ($8.7 \times 10^{10}\,M_\odot$) and SFR ($85\,M_\odot\,{\rm yr}^{-1}$).
3. In comparison with other samples, the CO properties suggests that J100054 is similar to star-forming galaxies at $z \sim 1$.

We thank the referee for constructive feedback that helped us improve the paper. We acknowledge useful discussions with Andrew Baker and George Privon. CHILES is supported by NSF grants AST-1413102, AST-1412578, AST-1412843, AST-1413099 and AST-1412503. X.F. is supported by an NSF-AAPF under award AST-1501342. L. C. and E.T. acknowledge support from NSF grant AST-1412549. K.H. was supported by the ERC under the EU's Seventh Framework Programme (FP/2007-2013)/ERC Grant Agreement nr. 291531. K.K. acknowledges grants KR 4598/1-2 and SCHI 536/8-2 from the DFG Priority Program 1573. Y. J. acknowledges the Marie Curie Actions of the European Commission (FP7-COF). This work would not have been possible without the long-term financial support from the Mexican Science and Technology Funding Agency, CONACYT during the construction and early operational phase of the Large Millimeter Telescope Alfonso Serrano, as well as support from the the US NSF via the URO program, the INAOE and UMASS-Amherst. Based on observations obtained at the SOAR telescope, which is a joint project of the MCTI da República Federativa do Brasil, NOAO, UNC-Chapel Hill, and MSU.

REFERENCES

Arnouts, S., Cristiani, S., Moscardini, L., et al. 1999, MNRAS, 310, 540
Bauermeister, A., Blitz, L., Bolatto, A., et al. 2013, ApJ, 768, 132
Bolatto, A. D., Wolfire, M., & Leroy, A. K. 2013, ARA&A, 51, 207
Capak, P., Aussel, H., Ajiki, M., et al. 2007, ApJS, 172, 99
Catinella, B., & Cortese, L. 2016, MNRAS, 446, 3526
Catinella, B., Schiminovich, D., Kauffmann, G., et al. 2012, A&A, 544, A65
Chang, T.-C., Pen, U.-L., Bandura, K., & Peterson, J. B. 2010, Natur, 466, 463
Chung, A., van Gorkom, J. H., Kenney, J. D. P., Crowl, H., & Vollmer, B. 2009, AJ, 138, 1741
Chung, A., Yun, M. S., Naraynan, G., Heyer, M., & Erickson, N. R. 2011, ApJL, 732, L15
Cybulski, R., Yun, M. S., Erickson, N., et al. 2016, MNRAS, 459, 3287
Davies, L. J. M., Robotham, A. S. G., Driver, S. P., et al. 2015, MNRAS, 452, 616
Delhaize, J., Meyer, M. J., Staveley-Smith, L., & Boyle, B. J. 2013, MNRAS, 433, 1398
Downes, D., & Solomon, P. M. 1998, ApJ, 507, 615
Erickson, N., Narayanan, G., Goeller, R., & Grosslein, R. 2007, in ASP Conf. Ser. 375, From Z-Machines to ALMA: (Sub)Millimeter Spectroscopy of Galaxies, ed. A. J. Baker et al. (San Francisco, CA: ASP), 71
Eskew, M., Zaritsky, D., & Meidt, S. 2012, AJ, 143, 139
Fernández, X., van Gorkom, J. H., Hess, K. M., et al. 2013, ApJL, 770, L29
Gao, Y., & Solomon, P. M. 2004, ApJS, 152, 63
Geach, J. E., Smail, I., Moran, S. M., et al. 2011, ApJL, 730, L19
Geréb, K., Morganti, R., Oosterloo, T. A., Guglielmino, G., & Prandoni, I. 2013, A&A, 558, A54
Haynes, M. P., Giovanelli, R., & Chincarini, G. L. 1984, ARA&A, 22, 445
Hopkins, A. M., & Beacom, J. F. 2006, ApJ, 651, 142
Huang, S., Haynes, M. P., Giovanelli, R., et al. 2014, ApJ, 793, 40
Ilbert, O., Arnouts, S., McCracken, H. J., et al. 2006, A&A, 457, 841
Kartaltepe, J. S., Sanders, D. B., Le Floc'h, E., et al. 2010, ApJ, 721, 98
Koekemoer, A. M., Aussel, H., Calzetti, D., et al. 2007, ApJS, 172, 196
Kroupa, P. 2001, MNRAS, 322, 231
Lah, P., Chengalur, J. N., Briggs, F. H., et al. 2007, MNRAS, 376, 1357
Le Floc'h, E., Aussel, H., Ilbert, O., et al. 2009, ApJ, 703, 222
Lee, C., Chung, A., Yun, M. S., et al. 2014, MNRAS, 441, 1363
Lutz, D., Poglitsch, A., Altieri, B., et al. 2011, A&A, 532, A90
Maddox, N., Hess, K. M., Obreschkow, D., Jarvis, M. J., & Blyth, S.-L. 2015, MNRAS, 447, 1610
Magnelli, B., Ivison, R. J., Lutz, D., et al. 2015, A&A, 573, A45
Massey, R., Stoughton, C., Leauthaud, A., et al. 2010, MNRAS, 401, 371
Masui, K. W., Switzer, E. R., Banavar, N., et al. 2013, ApJL, 763, L20
Murphy, E. J., Condon, J. J., Schinnerer, E., et al. 2011, ApJ, 737, 67
Oliver, S. J., Wang, L., Smith, A. J., et al. 2010, A&A, 518, L21
Rodighiero, G., Daddi, E., Baronchelli, I., et al. 2011, ApJL, 739, L40
Saintonge, A., Kauffmann, G., Kramer, C., et al. 2011, MNRAS, 415, 32
Sargent, M. T., Daddi, E., Béthermin, M., et al. 2014, ApJ, 793, 19
Schinnerer, E., Smolčić, V., Carilli, C. L., et al. 2007, ApJS, 172, 46
Scoville, N., Sheth, K., Walter, F., et al. 2015, ApJ, 800, 70
Scudder, J. M., Ellison, S. L., Torrey, P., Patton, D. R., & Mendel, J. T. 2012, MNRAS, 426, 549
Sutherland, W., & Saunders, W. 1992, MNRAS, 259, 413
Tacconi, L. J., Neri, R., Genzel, R., et al. 2013, ApJ, 768, 74
U, V., Sanders, D. B., Mazzarella, J. M., et al. 2012, ApJS, 203, 9
Verheijen, M., van Gorkom, J. H., Szomoru, A., et al. 2007, ApJL, 668, L9
Walter, F., Brinks, E., de Blok, W. J. G., et al. 2008, AJ, 136, 2563
Zwaan, M. A., van Dokkum, P. G., & Verheijen, M. A. W. 2001, Sci, 293, 1800